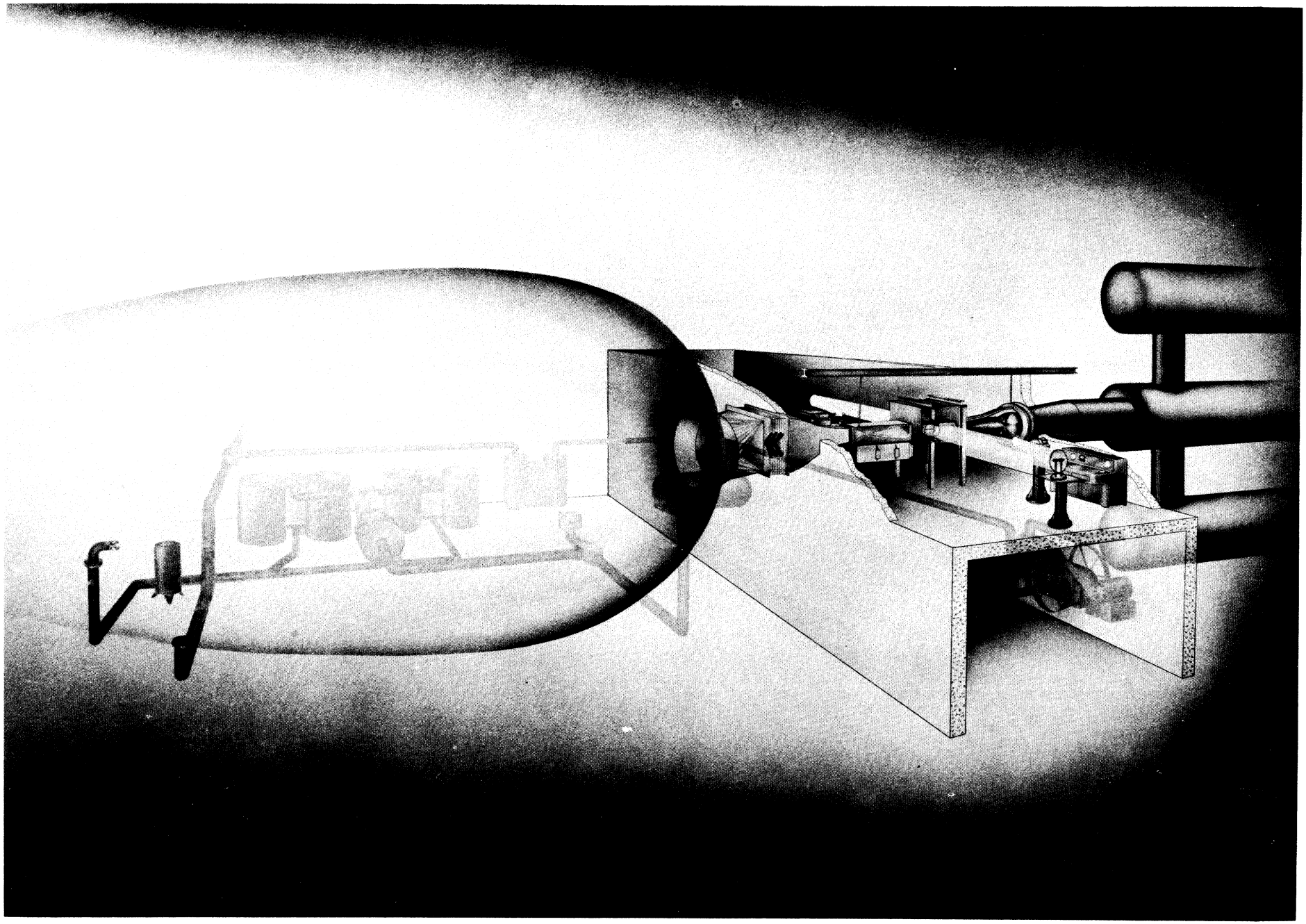

Artist's View of 8 x 13-inch Supersonic Wind Tunnel Installation

CALIBRATION REPORT

ON THE

UNIVERSITY OF MICHIGAN SUPERSONIC WIND TUNNEL

PART III. AERODYNAMIC CALIBRATION AT NOMINAL MACH NUMBER OF 2.84

PART IV. AERODYNAMIC CALIBRATION AT NOMINAL MACH NUMBER OF 1.44

By

P. E. CULBERTSON
Research Associate

Approved by

H. P. LIEPMAN, Wind Tunnel Director

WTM-213
(Supplement to UMM-36)

Project D-92

ENGINEERING RESEARCH INSTITUTE
UNIVERSITY OF MICHIGAN
ANN ARBOR

June, 1952

UNP0916

TABLE OF CONTENTS

INTRODUCTION

This report is the first supplement to the basic calibration report (UMM-36) of the 8 x 13-inch supersonic wind tunnel of the Department of Aeronautical Engineering at the University of Michigan. The aerodynamic calibration of the flow in the test section is presented for nozzle blocks with nominal Mach numbers of 2.84 and 1.44, respectively. By publication time calibration tests on the Mach 2.5 nozzle and exploratory tests on the Mach 4 nozzle will have been completed. Results of these calibrations will be published later.

PART III

AERODYNAMIC CALIBRATION AT NOMINAL MACH NUMBER OF 2.84

Summary

The nozzle blocks used in this calibration were designed for an outlet Mach number of 3.0 in accordance with the analytical method derived by Kuno Foelsch. The perfect fluid nozzle contours have been corrected for boundary-layer buildup on the contoured surfaces by the method of Reference 1.

A Mach number of 2.84 was determined experimentally at the center of the test section. Flow conditions correspond to a Reynolds number of approximately 2.76×10^6 per foot.

From 7 inches upstream to 8 inches downstream of the test-section center, the Mach number varies from 2.81 to 2.86.

The ratio of stagnation pressure in the test section to atmospheric pressure is 0.96 at a stagnation dew point of -25°F. This indicates a stagnation pressure loss of approximately 0.59 psi.

Flow inclination, both horizontal and vertical, is $0 \pm 0.18°$ from the geometric zero, with a standard deviation of 0.07°.

Maximum length of run for the Mach 2.84 configuration was found to be approximately 19 seconds. This length of run requires about 28 minutes of pumping time.

The allowable test dew point was found to be about -5°F.

1. Pressure and Mach-Number Distribution

The flow in the test section was calibrated by means of static- and total-pressure probes, the flow inclinometer, and schlieren observation. Because of the small absolute value of the static pressure at Mach 2.84, mercury manometry was considered to be of insufficient accuracy. All static pressures

were therefore measured by differential oil manometry. Statistical evaluation of static-pressure data for two wall orifices gave a probable error of ± 0.0003 in the measurement of static to atmospheric pressure ratio. Because of the limited availability of manometers suitable for oil, no sidewall pressures were taken, and only single-needle probes were utilized.

From the test data the following observations can be made:

a) The shock waves visible in the test section (Fig. III-1) can be traced upstream to the immediate vicinity of the nozzle—test-section juncture. Since no sidewall pressures were taken, it is not known if these shocks come from the nozzle and reflect at the juncture, or originate at the juncture. The latter possibility is believed to be most likely. The two major shock waves appear to be of about equal strength; the flow inclination data show that the combination of the two and all other disturbances produces negligible inclination along the axial centerline of the tunnel.

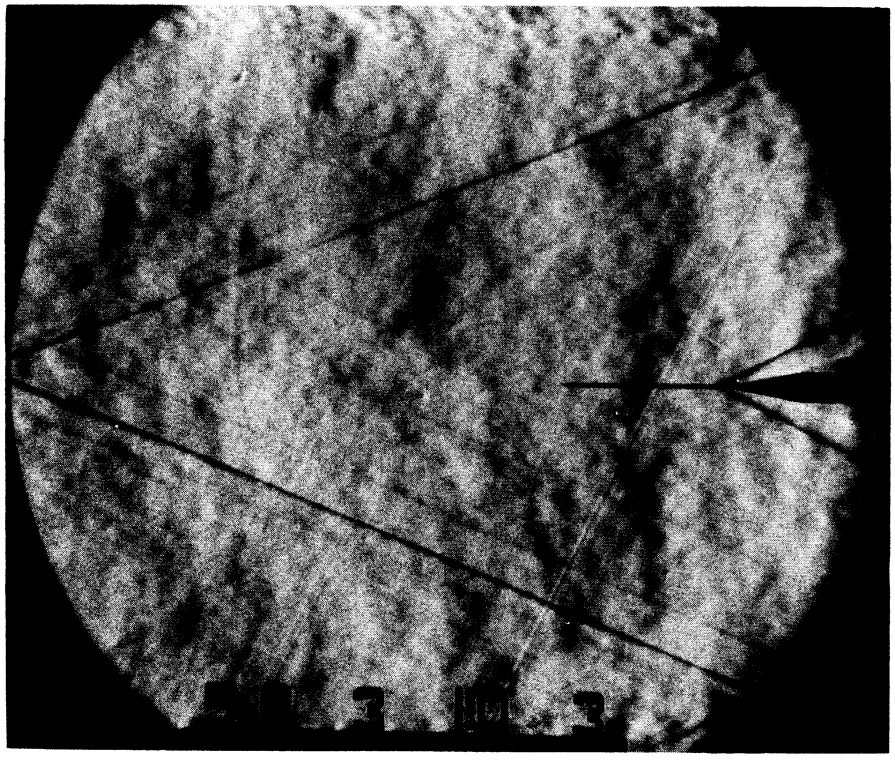

Fig. III-1. Mach 2.84 flow in test section with static needle probe.

Both static- and total-head probes were used in an attempt to determine the strength of the strongest shock wave reflected through the test section from the upper tunnel wall. Because of the effect of the intersection of the shock wave and the probe on the pressure at the static orifice, the static

pressure measurements are considered less valid than those obtained by the total-head probe. The results of the survey, made where the free-stream Mach number upstream of the shock was 2.85, indicated a Mach-number loss through the shock wave of 0.04, which is associated with a flow deflection of 0.8°. The angle of the shock wave could not be determined with sufficient accuracy to confirm these values because of local disturbances and the spanwise averaging effect.

No measures were taken at this time to eliminate or reduce these shocks, since a sufficiently large undisturbed test-section region is available with the present nozzle.

b) Concurrent with the visible shock waves, expansion regions, which are not visible in the schlieren photographs, exist on the axial centerline. As seen in Fig. III-2, this expansion extends from about 2 inches upstream to 7 inches downstream of the test-section center, and is of sufficient strength to overcome the usual pressure increase because of the boundary-layer growth.

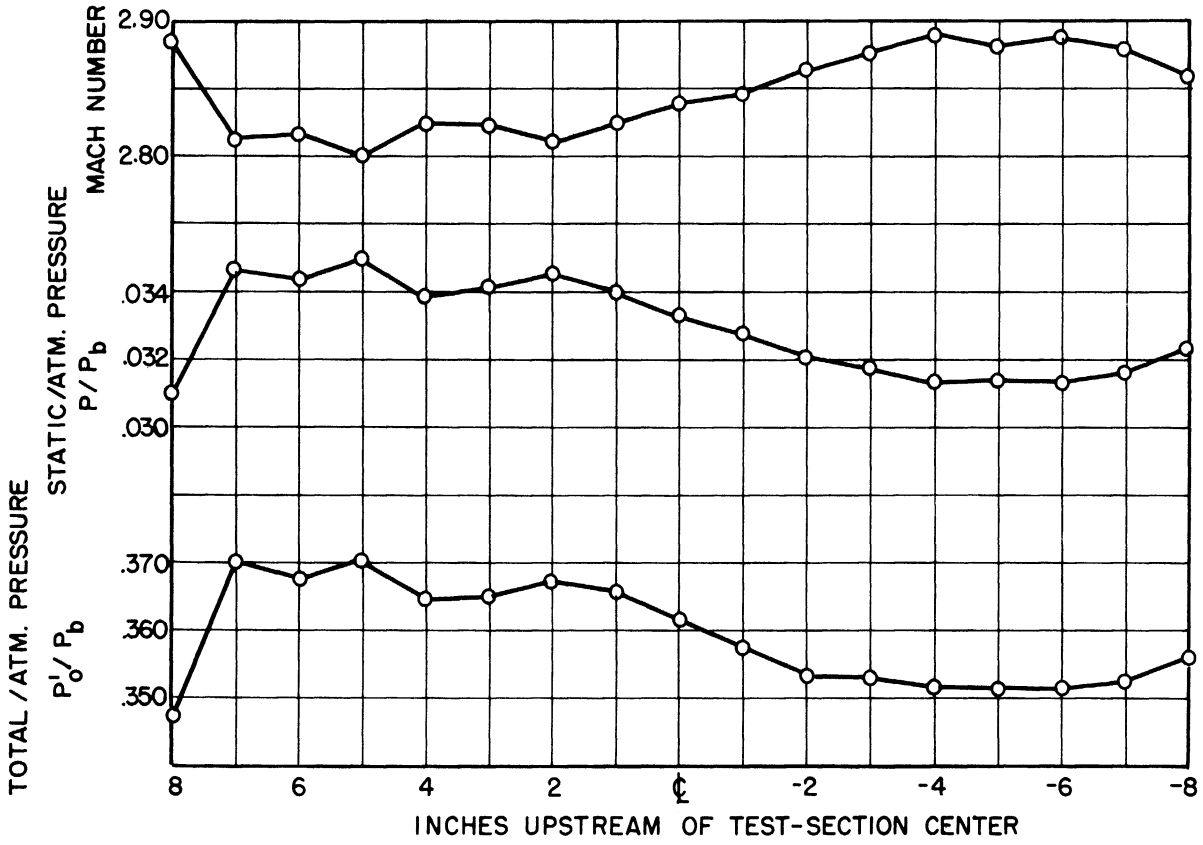

Fig. III-2. Mach number and pressure gradients on axial centerline.

c) The fact that significant axial pressure gradients exist in the flow without appreciable inclination along the centerline (see Fig. III-3)

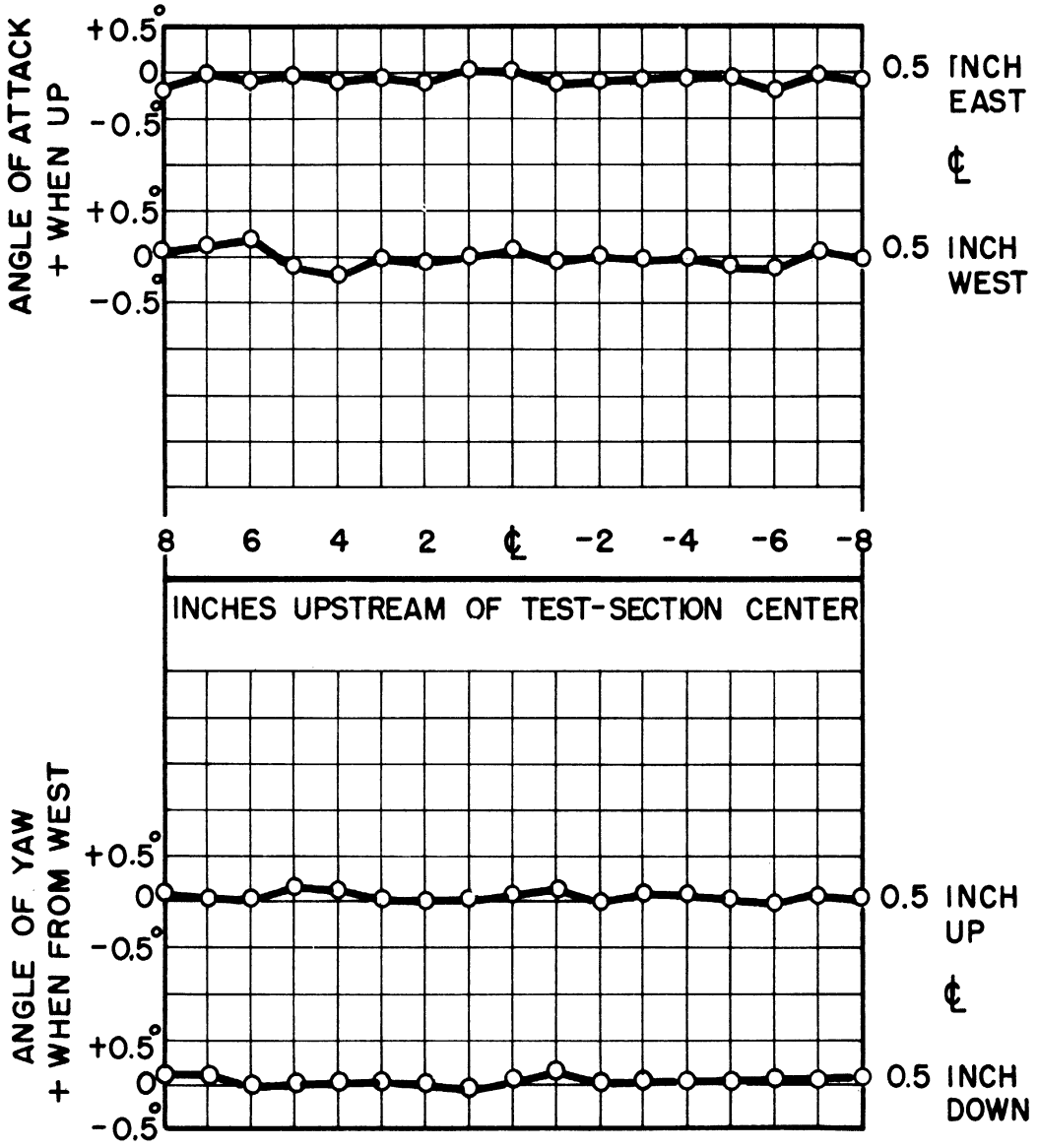

Fig. III-3. Flow inclination data.

indicates that the flow is relatively symmetrical about horizontal and vertical planes through the axial centerline.

d) The experimental static- and total-head pressure ratios have been used to calculate the Mach number from the equation

$$\frac{p_o'/p_b}{p/p_b} = \left[\frac{2\gamma M^2 - (\gamma-1)}{\gamma+1}\right]^{1/(1-\gamma)} \left[\frac{(\gamma+1)\,M^2}{2}\right]^{\gamma/(\gamma-1)},$$

where p_b is the pressure in the storage bag, equal to atmospheric pressure.

With this Mach number and the equation

$$\frac{p_o}{p_o'} = \left[\frac{2\gamma M^2 - (\gamma-1)}{\gamma+1}\right]^{1/(1-\gamma)} \left[\frac{(\gamma+1)\,M^2}{2 + (\gamma-1)\,M^2}\right]^{\gamma/(\gamma-1)},$$

a relationship between p_o at the test point and p_b (atmospheric pressure) can be found. A mean value of $p_o/p_b = 0.96$ has been calculated in this manner. This indicates a stagnation pressure loss of 0.59 psi between the storage bag (at atmospheric pressure) and the test section.

e) In connection with another test program, total/atmospheric pressure data have been taken across half the width of the test section 0.776 inch upstream of the test-section center. These data, shown in Fig. III-4 below, were taken with orifices in the blunt leading edge of an airfoil, 6% thick, spanning the entire width of the tunnel. Each point on this figure represents data taken at angles of attack of 0°, ± 2°, ± 4°, ± 6°, and ± 8°.

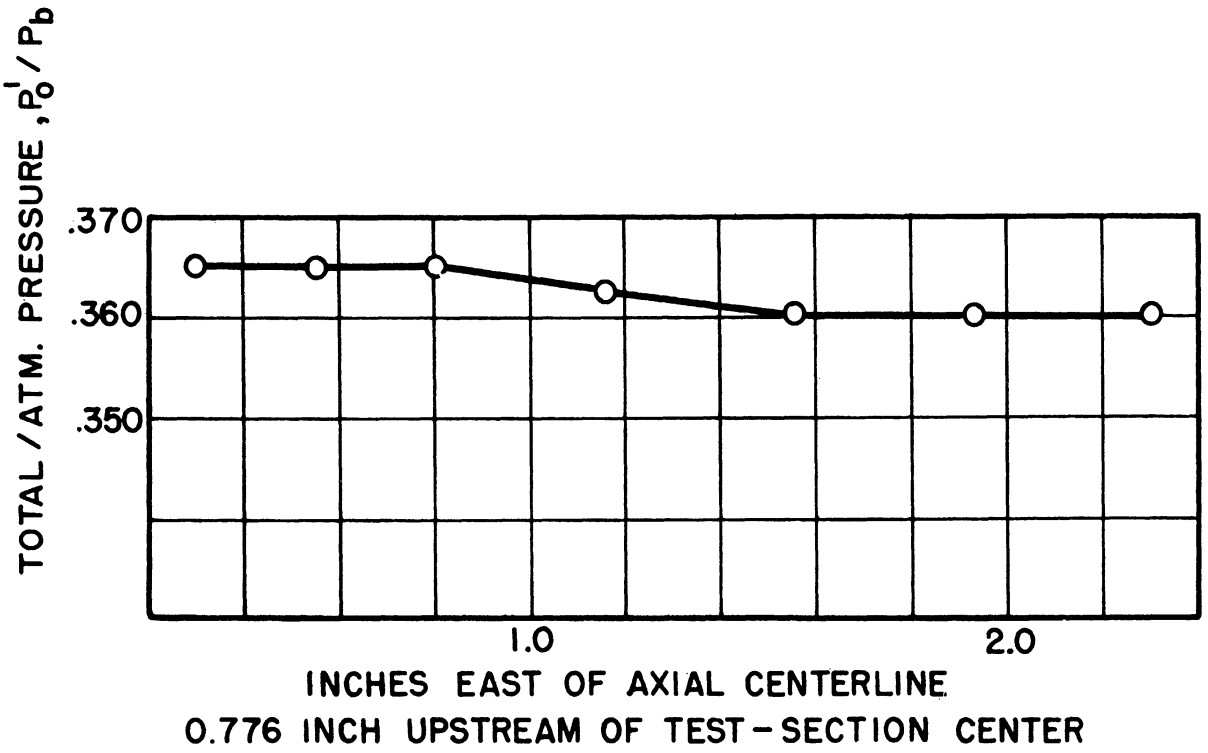

Fig. III-4. Spanwise distribution of total/atmospheric pressure.

Total/atmospheric pressure as measured by a blunt, full-spanning probe at 2° increments of angle of attack between +8° and -8° at an axial station 0.776 inch upstream of the test-section center.

2. Flow Inclination

The flow inclination was measured with the probe described in Reference 2 after it had been modified to permit manometer stabilization in the length of time available during a run. This was done by increasing the inside diameter of the pressure lead from 0.028 inch to 0.048 inch. The internal construction prohibited the use of more than four tubes; therefore, the inclination was measured at only two locations during each run. As shown in Fig. III-3, these points are 0.5 inch on each side of the centerline of the probe.

The results, presented in Fig. III-3, show that the flow inclination on the axial centerline is $0 \pm 0.18°$, with a standard deviation from 0 to 0.07°, with the exception of the one point 6 inches upstream of the centerline. In this position the upper wedge intercepts some of the minor shock waves (Fig. III-5) and the static-pressure data are likely to be less accurate because of the shock-wedge and wedge—boundary-layer interactions.

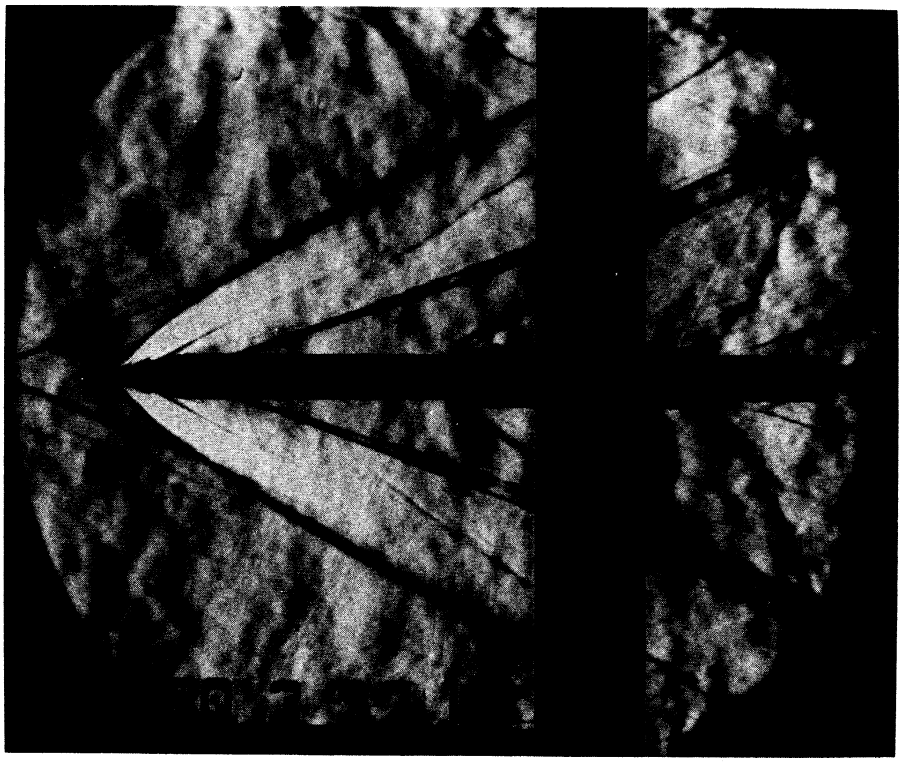

Fig. III-5. Flow inclination probe in Mach 2.84 flow.

Since probing was limited to the immediate neighborhood of the tunnel axis, the data establish only the symmetry of the shock and expansion disturbances noted in the test section.

3. Blocking

No systematic tests were made of the blocking characteristics of the Mach 2.84 flow because of the limited time available for the calibration. Furthermore, most models tested at Mach 2.84 will also be tested at Mach 1.90, where model size is more critical. It was found, however, that a cone cylinder of 20° half-angle and 3 inches in diameter did not block the flow at a 10° angle of attack, whereas the same model blocked the Mach 1.9 flow at a 0° angle of attack.

4. Length of Run

The length of run is considered to be the period between the downstream passage of the initial normal shock wave and the breakdown of supersonic flow.

The duration of supersonic flow in the test section as a function of the initial pressure ratio is shown in Fig. III-6. The theoretical values of length of run shown in this figure are based on the equation given in Reference 2, and differ from the experimental values because of the diffusion characteristics of the tunnel. These runs were made with a cone-cylinder in the test section and with the inner body of the diffuser at its optimum position. The corresponding throat area of the diffuser at this position is 105 square inches, which is small enough to trap the shocks effectively. When the shocks are trapped in this way, there is no visual evidence of the transient oblique shock waves which appears in the test section at the Mach 1.90 nozzle just prior to the complete breakdown of supersonic flow.

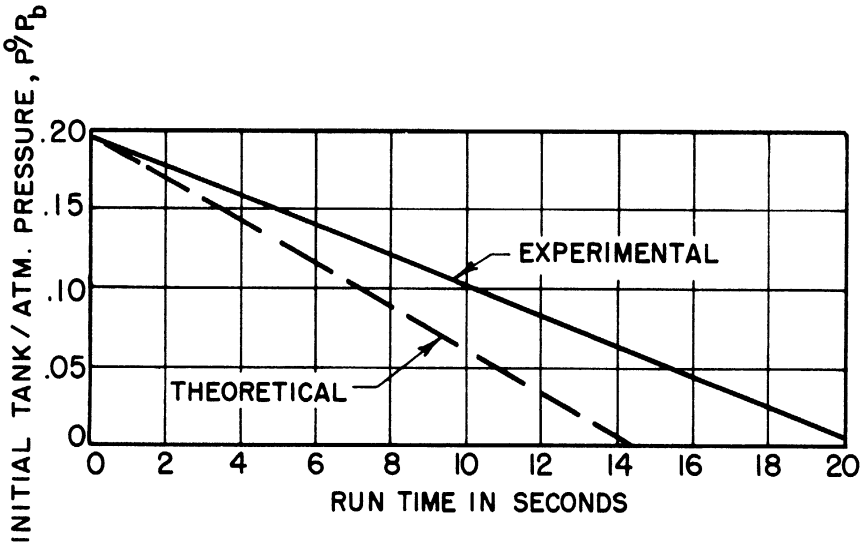

Fig. III-6. Length of run.

By correlating these data with the characteristics of the vacuum pump, Fig. III-7 is obtained, showing the pumping time required to evacuate the vacuum tanks from the pressure at the end of a run to the pressure required for a subsequent run of given duration.

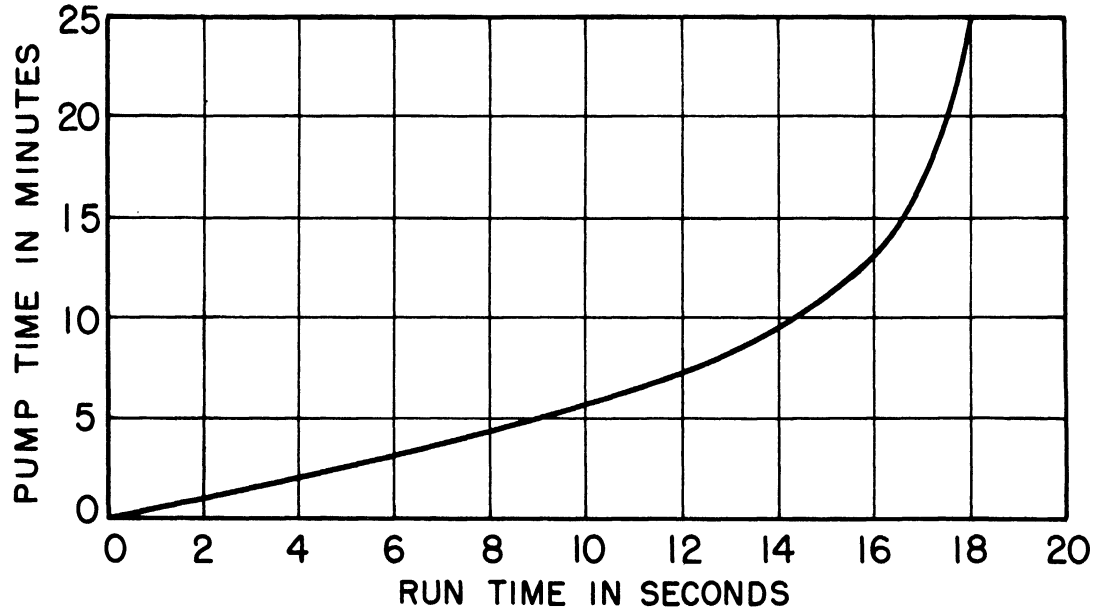

Fig. III-7. Pumping time.

5. Influence of Humidity

Although theoretical work indicates that certain compensations can be made for the presence of water vapor in the test air, the use of such corrections is, as described in Reference 2, extremely limited. It is, however, possible to confirm theoretically the amount of water vapor which has been found experimentally to be tolerable. The criterion which has been established is that for satisfactory test conditions the increase in pressure due to the influence of a condensation shock must be less than the inaccuracies due to the pressure measuring techniques used in testing. If, therefore, pressure measurements are made under near-ideal conditions and the stagnation dew point is varied, a statistical study will yield a dew point above which the increase in pressure due to the humidity cannot be tolerated under the established criteria. Fig. III-8 shows the results of such a study at a point 3 inches upstream of the test-section center, where the Mach number is 2.82. The theoretical curve was based on the theory utilized in Reference 3, which assumes that 90°F of supercooling takes place before the condensation shock occurs. Although this assumption is not rigorously correct, it appears to confirm the experimental results to the accuracy required.

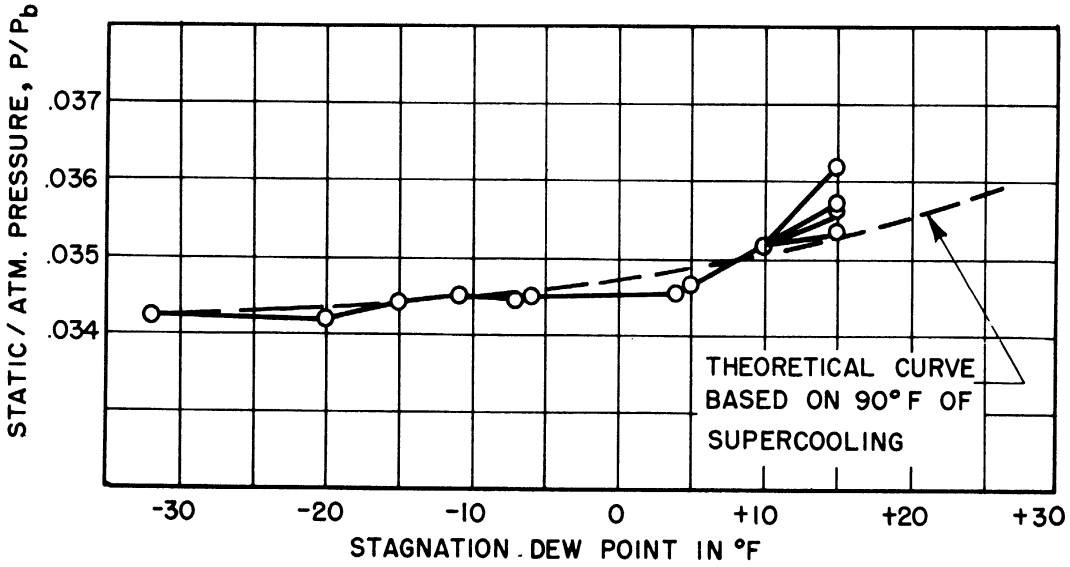

Fig. III-8. Influence of humidity as measured by static probe on centerline of tunnel.

Using the value of $\pm$ 0.0003 as the accuracy to which a static-pressure ratio p/p_b can be measured with oil manometry, the maximum stagnation dew point at which tests should be run is -5°F. This is called the "allowable test dew point". The vast majority of the calibration data, however, were obtained with stagnation dew points of less than -25°F.

PART IV

AERODYNAMIC CALIBRATION AT NOMINAL MACH NUMBER OF 1.44

Summary

The nozzle blocks used in this calibration were designed for an outlet Mach number of 1.5 by the analytical method of Kuno Foelsch. Boundary-layer corrections have been applied to the contoured surfaces in accordance with the method of Reference 1.

The Mach number of the flow at the center of the test section was experimentally found to be 1.44. Flow conditions correspond to a Reynolds number of approximately 4.86×10^6 per foot.

In the test rhombus, i.e., between the test-section center and 10 inches upstream, the Mach number varies between 1.42 and 1.48.

The ratio of stagnation pressure in the test section to atmospheric pressure is 0.998 at a stagnation dew point of -25°F.

Flow inclination in the test rhombus varies between extremes of +0.1° and -0.04° in angle of attack and from +0.7° to -0.3° in angle of yaw.

Length of run was found to be essentially linear with vacuum-tank pressure, with a maximum of approximately 19 seconds. This length of run requires approximately 26 minutes of pumping time.

The allowable test dew point was found to be -20°F.

1. Pressure and Mach-Number Distribution

The pressure and Mach-number distributions were determined in a manner similar to that described in Reference 2; they are presented in Figs. IV-1 to IV-3. For this calibration, mercury manometry and the 5-prong probes were utilized. A new cantilevered support strut was used when it was found that the existing full-spanning struts blocked the tunnel. The location of

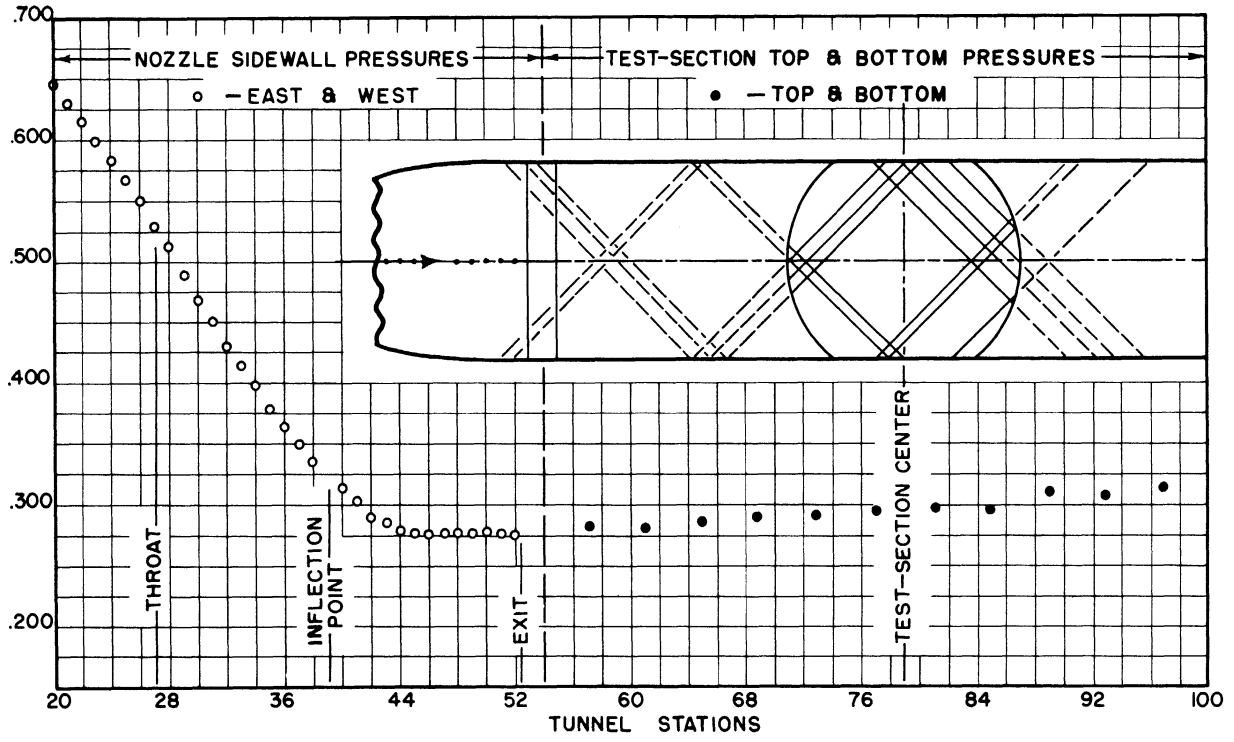

Fig. IV-1. Static wall pressures and shock pattern for the Mach 1.44 nozzle.

this strut permitted probing forward of the test-section center only; however, one complete rhombus was studied.

Evaluation of the pressure data taken leads to the following conclusions:

a) Shock waves are visible in the test section, which, when extrapolated upstream, are seen to have originated, or reflected, at the juncture of nozzle exit and test section (station 52.5). Fig. IV-1 shows this shock pattern and also the static pressures along the center of the nozzle sidewalls and top and bottom of the test section. This figure and the corresponding data for the M = 1.90 nozzle (Fig. II-5 of Reference 2) show good agreement between the top and bottom pressures and the shock patterns downstream of the nozzle—test-section juncture. The sidewall pressures at the nozzle exit indicate an expansion which agrees with the physical picture of the nozzle exit deflecting under load and creating a step-down juncture between it and the test section. This expansion is then followed by shocks as the flow turns parallel to the test section. The possibility that the visible shocks originate in the nozzle itself and then reflect near the juncture is not borne out by the nozzle-sidewall pressure data.

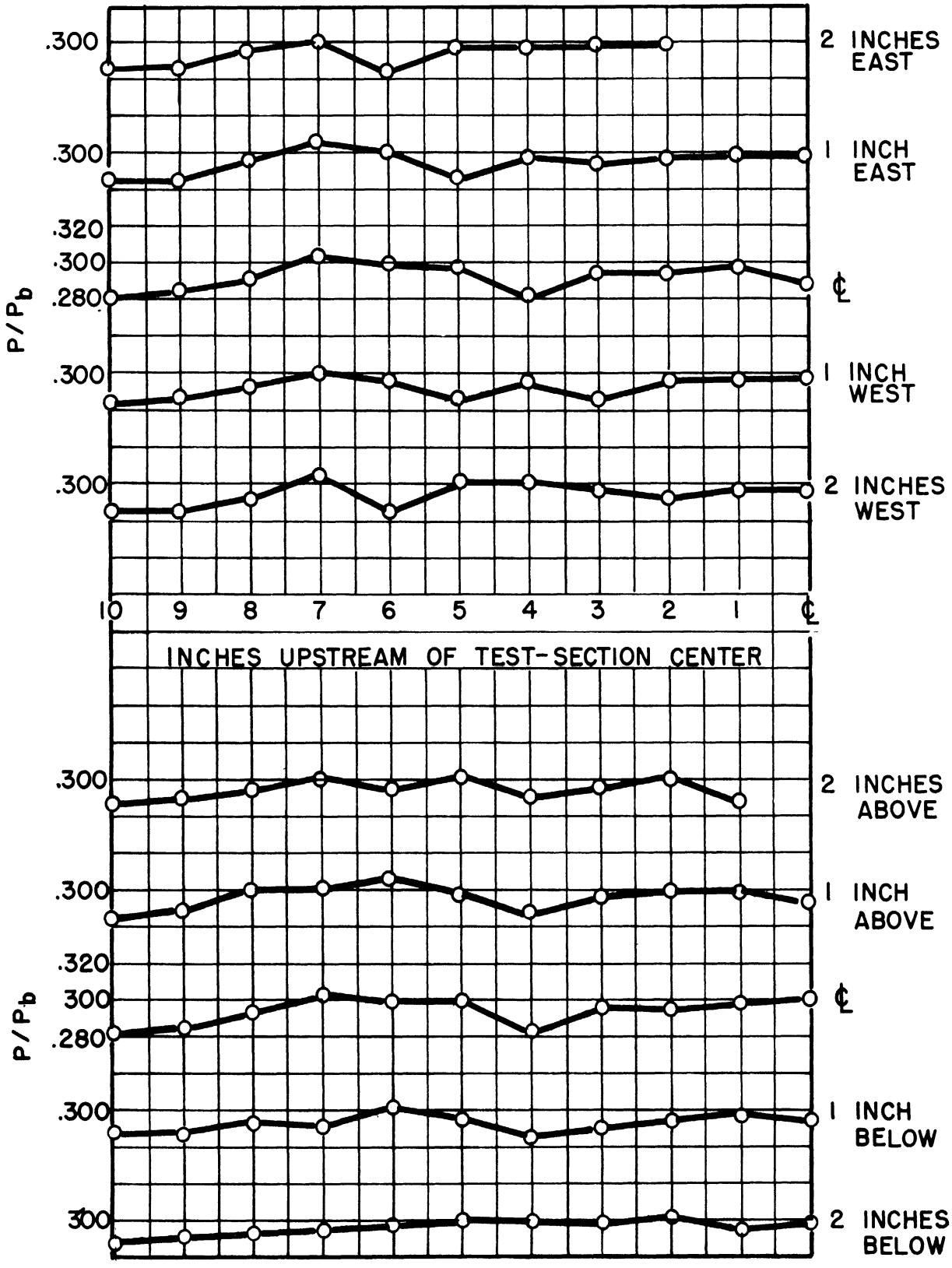

Fig. IV-2. Static/atmospheric pressure ratio.

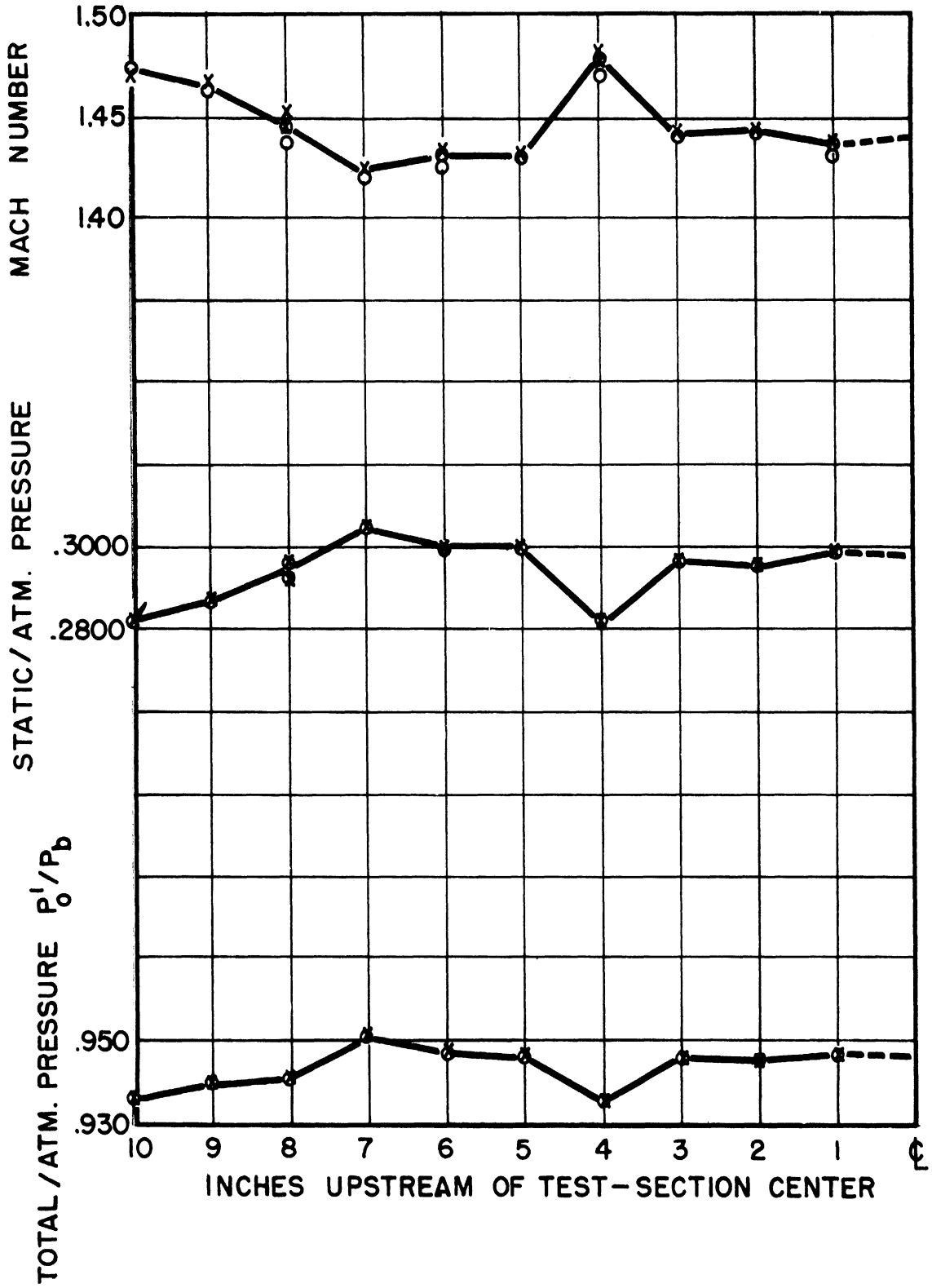

Fig. IV-3. Mach number and pressure gradients on axial centerline.

The shock pattern in the test section is also noticeable in the pressure data taken with the 5-prong probes (Figs. IV-2 and IV-3) as they cross the axial centerline between 6 and 10 inches upstream of the test-section center.

b) Two relatively symmetric shocks originate on the test-section sidewalls, near the juncture of window, window frame, and sidewall, and cross the centerline about 4 inches upstream of the test-section center. These shocks and associated expansions are detected in the pressure data of Figs. IV-2 and IV-3 and can be seen in Fig. IV-4, where they intersect the window in a typical curved trace, and in Fig. IV-5, where their reflection, just upstream of the cone-cylinder junction of the model, is visible as well as the window intersection in the top and bottom regions of the picture. (The shocks originating near the rear quarter of the cylinder are caused by horizontal fins not visible in the schlieren.)

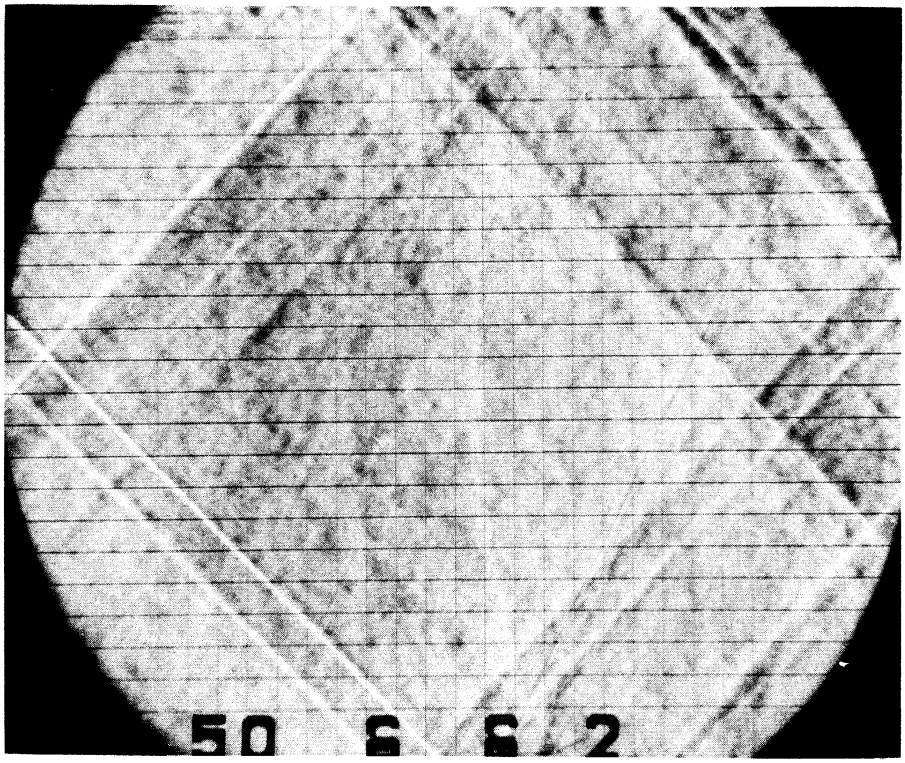

Fig. IV-4. Mach 1.44 flow in test section.

Since completion of this analysis, the junctures between sidewall, window frame, and window have been smoothed. These shocks have therefore been considerably reduced in strength if not completely eliminated.

c) The distribution of Mach number and static pressure along the axial centerline of the tunnel (Fig. IV-3) shows also that the expansion region between the test-section center and 6 inches upstream is sufficiently

strong to override the static-pressure increase (or Mach-number decrease) caused by boundary-layer buildup along the walls.

d) Following the method described in section 1-d of the preceding Calibration Report, an average value of $p_o/p_b = 0.998$ was calculated. This corresponds to a stagnation pressure loss of approximately 0.03 psi between the storage bag and the test section.

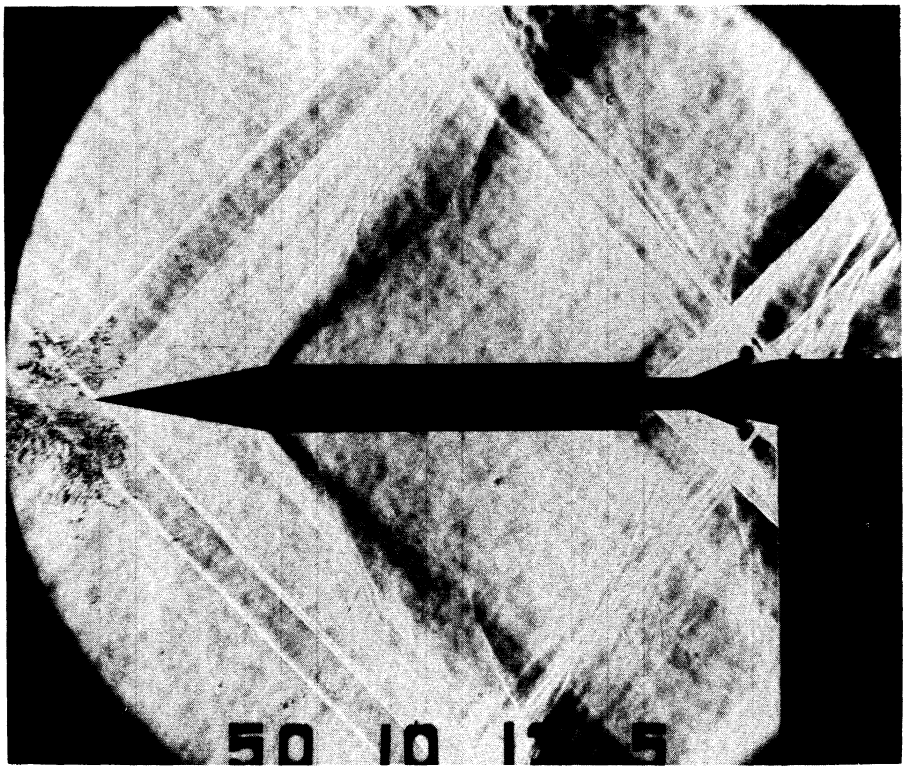

Fig. IV-5. Cone-cylinder model in Mach 1.44 flow.

2. Flow Inclination

The flow inclination was measured with the wedge described in Reference 2. The results are shown in Fig. IV-6. The data show that the effective angle of attack varies between extremes of +0.1° and -0.4°, while the effective yaw varies between extremes of +0.7° and -0.3°. The difficulty of determining the geometric yaw angle of the wedge accurately, however, limited the accuracy to which the effective yaw of the flow could be measured to ±0.2°, while it is felt that pitch could be determined to within ±0.1°. The flow inclination data of Fig. IV-6 show the general trends of the flow in the presence of the shocks originating from the nozzle—test-section juncture and the window-sidewall juncture. The location of these shocks in the flow inclination data is not as definite as in the pressure and schlieren data. This is

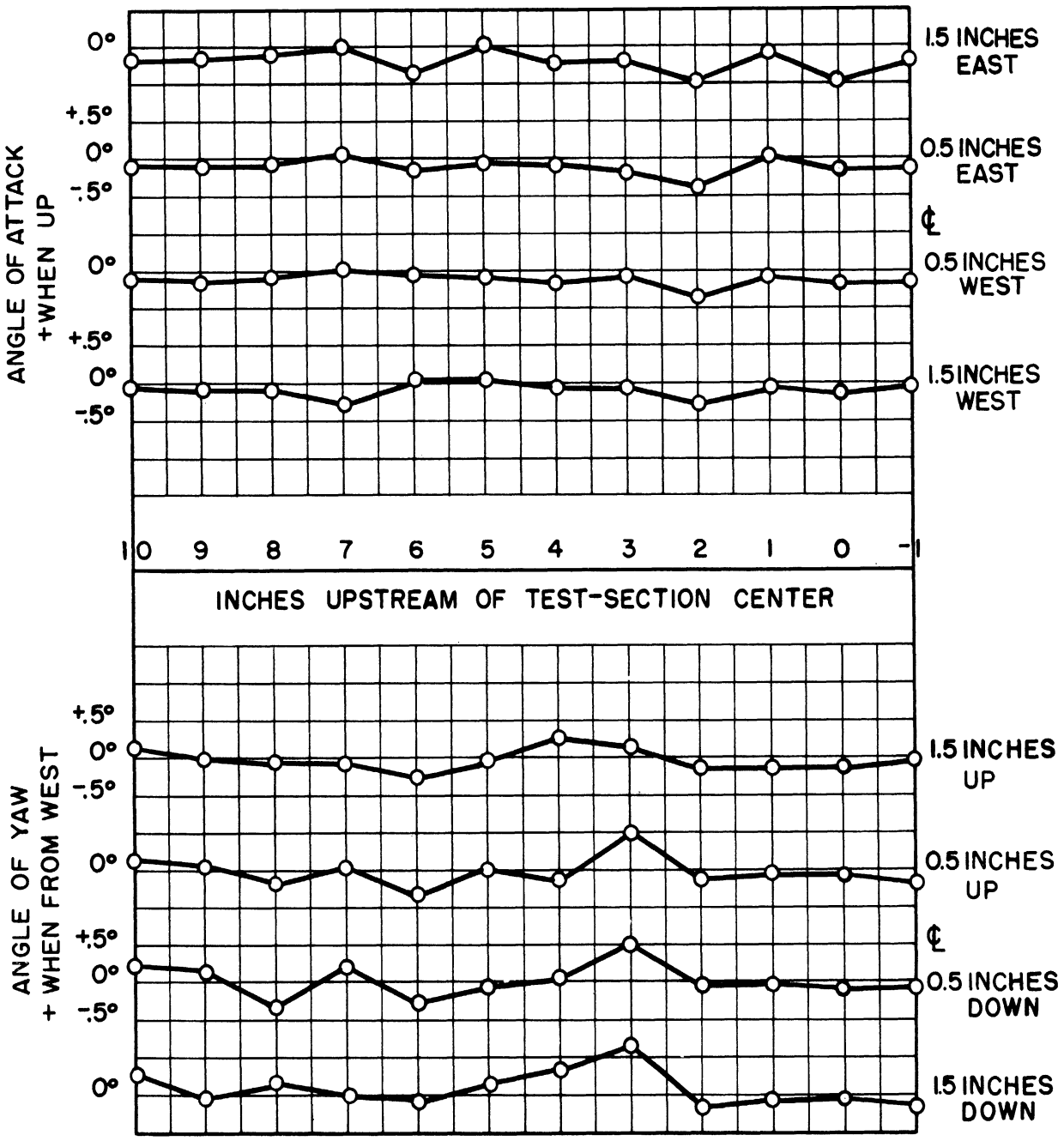

Fig. IV-6. Flow inclination data.

not unusual, since the flow inclination is obtained from static-pressure data on a wedge. Thus, inaccuracies can be expected whenever the wedge probes a region containing shocks because of the interaction between shocks and the wedge boundary layer and its effect on the static-pressure measurement.

This will also have a strong effect on the accuracies of the flow inclination measurements, especially if the disturbing shocks are unsymmetric with respect to the probing wedge. It is therefore possible that the extreme values and strong changes in measured flow inclination, especially between 2 to 4 inches and 6 to 9 inches upstream of the test-section center, are primarily due to this shock-wedge interaction rather than to the undisturbed flow. The subsequent smoothing of the sidewall-window juncture has probably reduced the yaw inclinations shown in Fig. IV-6 between 2 and 4 inches upstream of the test-section center.

3. Blocking

As mentioned in section 1 of this part, the vertical strut used for model support at other Mach numbers did not pass the flow. A cantilevered strut was therefore fabricated and utilized throughout the calibration.

It was found that cone-cylinder configurations of 3-inch diameter, 30° total apex angle, and 2-inch diameter, 40° total apex angle, blocked the flow, while a cone-cylinder of 2-inch diameter and 30° total apex angle passed the flow. A wing model of 7.75-inch span, 3.17-inch chord, 6% t/c mounted at 0° angle of attack on a sting 1.188 inches in diameter, also passed the flow. A similar wing section with a 40° total leading angle, producing a detached shock wave, mounted through the sidewall windows, passed the flow at a 4° angle of attack, but blocked the tunnel at 6°.

4. Length of Run

Theoretical and experimental values of the length of run obtainable are shown in Fig. IV-7 as a function of the vacuum-tank to atmospheric pressure ratio. The experimental values were obtained with a typical cone-cylinder model in the test section and the variable diffuser in its most open position. Fig. IV-8 shows the length of run plotted as a function of the time required to evacuate the vacuum tanks following a maximum-length run.

5. Influence of Humidity

Four sidewall orifice pressures were measured during runs of various stagnation dew points. The results of this study are presented in Fig. IV-9, showing a critical dew point of from -16°F to -20°F. The random scatter in the data at dew points in excess of -8°F illustrates the difficulty of obtaining a parameter whose use will compensate for excessively high dew points in a nonuniform stream. Theoretical computations of the influence of humidity

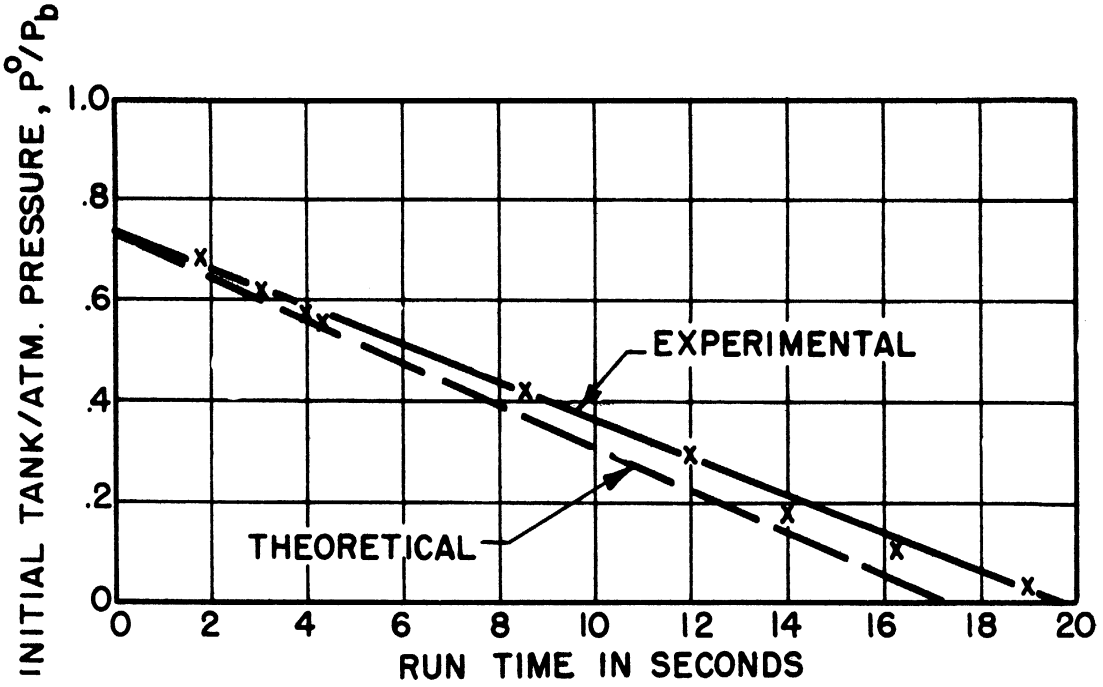

Fig. IV-7.

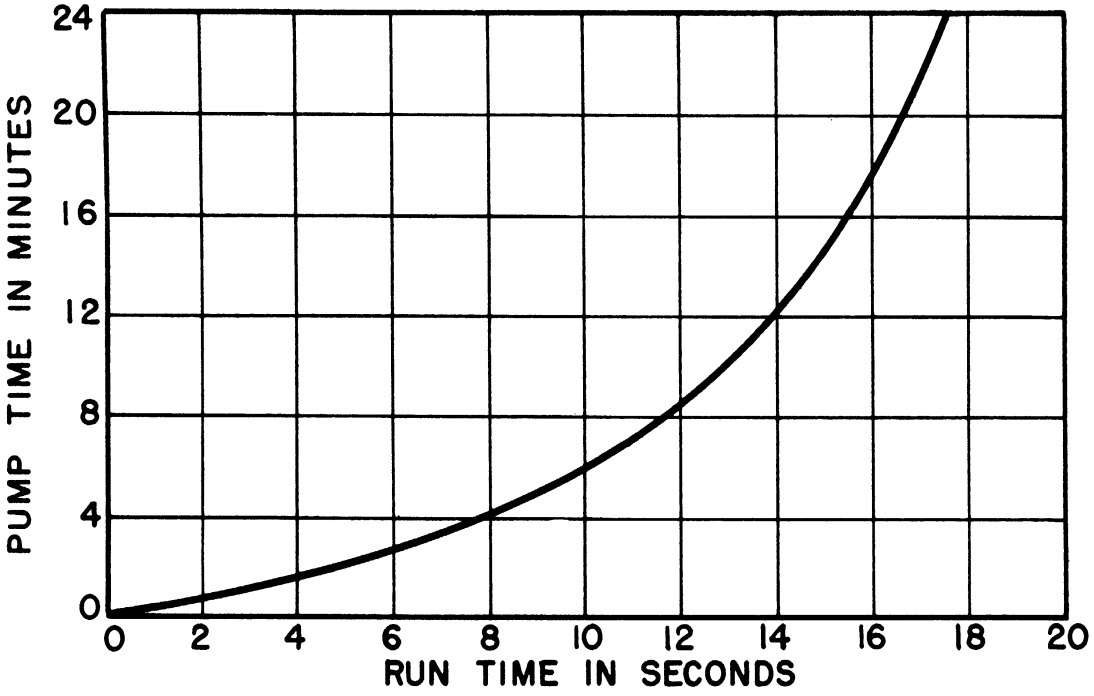

Fig. IV-8.

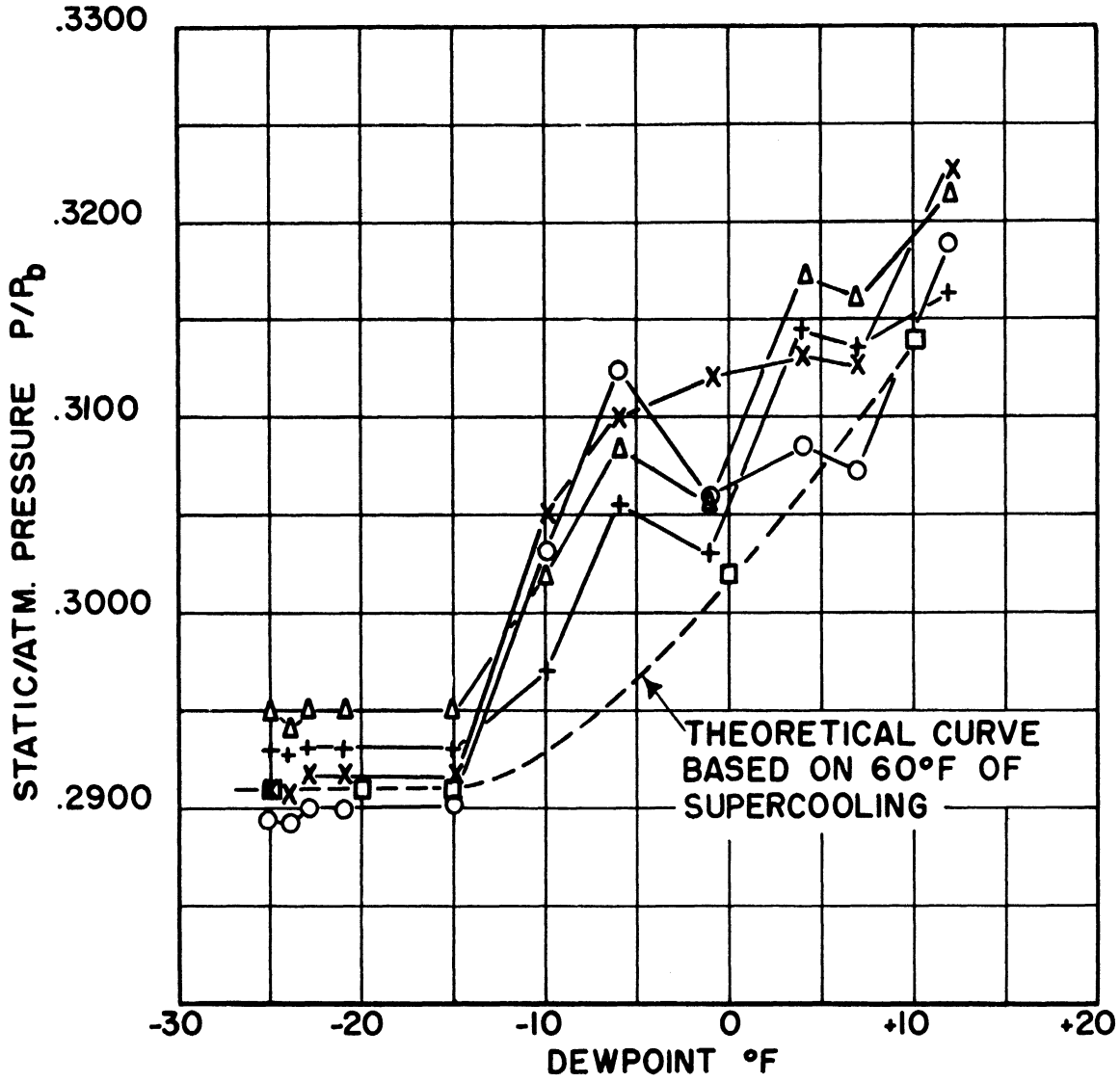

Fig. IV-9. Influence of humidity on static pressure as measured by four random wall taps.

presented in Reference 3 assumed 90°F of supercooling before condensation occurred. The flow through the supersonic region of the M = 1.44 nozzle, however, has a temperature gradient of approximately 0.75°C/cm, which is less than the figure of 1°C/cm usually considered the critical rate of temperature drop for the amount of supercooling to be independent of relative humidity and Mach number. Calculations based on 90° of supercooling lead to the result that at 0°F stagnation dew point, condensation would not occur until the flow reached a Mach number of 1.55. The experimental evidence indicates that 0°F is considerably higher than the critical value. The theory also indicates that the dew point becomes more critical for a given tunnel configuration as the test Mach number decreases, which means that the critical

dew point for M = 1.44 should be lower than the value of -15°F found at M = 1.90. In light of the experimental evidence, computations based on 60°F of supercooling indicate that with a stagnation dew point of -15°F condensation occurs at M = 1.45, resulting in a Mach-number decrease of 0.01 with an associated drop in static pressure of 1 per cent. It therefore seems relatively valid to assume approximately 60°F of supercooling for the M = 1.44 configuration, and to set the allowable test dew point at -20°F.

REFERENCES

1. Peterson, J.W., "Calibration of Boundary Layer Thickness in Expansive Supersonic Flow", University of Michigan Wind Tunnel Report IMB-46, 1947.

2. Culbertson, P.E., "Calibration Report on the University of Michigan Supersonic Wind Tunnel", UMM-36, November, 1949.

3. Frost, R.C., "Influence of Dew Point on the Mach Number and Pressure in the Test Section", WTM-116, August, 1949.